Microstructure, Deformation, and Fracture Behavior of Commercial ABS Resins

CELINA R. BERNAL,[1] PATRICIA M. FRONTINI,[1,*] MIGUEL SFORZA,[2] and MIGUEL A. BIBBÓ[3]

[1]Institute of Materials Science and Technology (INTEMA), University of Mar del Plata and National Research Council (CONICET), J. B. Justo 4302, 7600, Mar del Plata, [2]Monsanto Argentina SAIC, Ruta 12, Km 83.1, Zárate, and [3]Petroquímica Cuyo, J. D. Perón 646, Bs. As., Argentina

SYNOPSIS

The microstructure, deformation, and fracture behavior of commercial ABS resins were investigated. Fracture mechanics studies were carried out under both static and dynamic conditions. Fracture toughness was evaluated via the J-integral analysis. In addition static fracture experiments were conducted at different temperatures. The ABS resins assayed here exhibited different deformation and fracture behavior depending on loading mode, matrix molecular weight, strain rate, temperature, rubber content, and morphologies. The reasons for this material's behavior are discussed with the help of scanning and transmission electron microscopy (SEM and TEM) investigation methods. The major source of toughness seems to be matrix crazing and rubber cavitation under both static and dynamic experiences, but at low strain rates shear yielding also contributes to toughening. © 1995 John Wiley & Sons, Inc.

INTRODUCTION

ABS is a family of thermoplastics that contains three monomeric units: acrylonitrile, butadiene, and styrene. Typically, a styrene/acrylonitrile copolymer (SAN) matrix contains discrete butadiene-based elastomer particles for toughening. Elastomer particles are grafted with SAN to achieve necessary interaction with the matrix polymer. ABS is one of the most important rubber-toughened thermoplastics and is widely used for applications where toughness and surface gloss are important.

Both large and small rubber particles are present in commercial ABS. Therefore two different mechanisms are present in these materials: cavitation and concomitant shear and crazing. The small rubber particles are likely to produce cavitation and shear, while crazing will be initiated at large particles. Both processes are expected to contribute to toughness.

Fracture in rubber modified glassy polymers has been extensively investigated in the last two decades. More specifically a considerable effort was devoted to the analysis and evaluation of deformation and fracture behavior of ABS polymers. Both linear elastic[1-4] and elastic–plastic[5-7] fracture mechanics concepts have been considered. The applicability of either generally depends on the test conditions used, i.e., specimen geometry, temperature, and strain rate, because they determine whether the fracture behavior of a given material is brittle or ductile.

However, several questions remain unanswered and most features of their behavior remain unsolved. Recently, the influence of AN and rubber content upon mechanical behavior on model and commercial ABS thermoplastics have been discussed in several works.[8,9]

With the improvement and development in fracture mechanics techniques over the last few years, traditional methodologies have been questioned and modified. Using these new fracture mechanics techniques, crack initiation and crack growth can be evaluated by means of the whole J-R curve analysis.[10-13]

These techniques provide more accurate tools, especially for nonlinear fracture evaluation and J_C determination, which can modify and even change previous conclusions.

The present investigations were carried out on two groups of commercial grade ABS having differ-

* To whom correspondence should be addressed.

Journal of Applied Polymer Science, Vol. 58, 1–10 (1995)
 CCC 0021-8995/95/010001-10

ent matrix molecular weights and different rubber contents. Materials were tested under static and dynamic conditions. All samples displayed ductile behavior: under such conditions the J-integral seems to be the proper tool for the analysis of ductile fracture.

In addition, some studies regarding small and large strains were performed. Changes in the behavior of ABS resins were noted depending on loading mode, matrix molecular weight, strain rate, temperature, and rubber content. This material behavior was investigated with the help of scanning and transmission electron microscopy (SEM and TEM) methodologies.

EXPERIMENTAL

Materials and Specimen Preparation

Two groups of commercial grade ABS (acrylonitrile–butadiene–styrene terpolymer) type resins were investigated. The former group is an injection grade material series with different rubber contents: Lustran ABS 240, 440, 640, and 740. The latter group is an extrusion grade material series: Lustran ABS 252 and 452. Table I displays the materials' molecular data. Materials were provided by Monsanto Argentina SAIC.

Pellets of ABS resins were dried at 85°C for 2 h under vacuum and then compression molded at 190°C into thick plates suitable for subsequent mechanical characterization.

Bars for mechanical and fracture characterization were cut from the compression molded plaques and then machined to reach the final dimensions and improve edge surface finishing.

For fracture mechanics testing, sharp notches were introduced by a scalpel sliding a razor blade having an on-edge tip radius of 13 μm.

Microscopy

The microstructures of the investigated ABS materials were examined by TEM using ultrathin sections of compression molded specimens, stained by OsO_4. Numerical average diameters of the rubber inclusions were calculated from the micrographs using processing image PC software.

Fracture surfaces were examined by SEM (Jeol JSM 35 CF apparatus), after coating the broken surfaces with a thin gold layer.

Mechanical Characterization

Static mechanical characterization was carried out in a Shimadzu Universal S-500-C Testing Machine equipped with a thermostatic chamber that allows testing of the samples from −35 to 200°C.

Flexural moduli (E) were determined under ASTM standards. Uniaxial compression tests were performed on minicylindrical specimens (L/D close to 2 and D = 5 mm) deformed between lubricated plates. Uniaxial tension experiments were carried out on dumbbell specimens. Nominal tensile and compressive yield stresses, σ_{yt} and σ_{yc}, respectively, were taken as the maxima of the load-deflection curves.

All static mechanical tests were performed at 2 mm/min crosshead speed and room temperature.

Impact energy was determined at 3.5 m/s impact velocity, at room temperature using a ASTM D 256 pendulum. In addition two samples were also run in a Perkin–Elmer DMA 7e Dynamic Mechanical Analyzer at 1 Hz from 10 to 90°C.

Fracture Methodologies

J-resistance curves were determined by the multiple-specimen technique[10,11] consisting of loading a series of identical specimens to different amounts of crack extension and then unloading. The value of J for each specimen was determined from the

Table I Materials' Molecular Data

Material	Average Particle Diameter (μm)	Rubber Content (%)	Matrix Molecular Weight (g/mol)	Acrylonitrile Content (%)
ABS 240	0.15	10.6		27.3
ABS 440	0.14	15.5	100.000–120.000	24.4
ABS 640	0.14	18.0		24.5
ABS 740	0.14	23.1		24.2
ABS 252	0.15	10.6	160.000–180.000	26.7
ABS 452	0.15	15.6		25.0

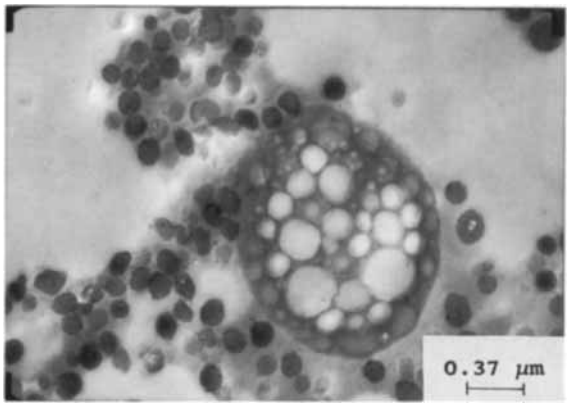

(a)

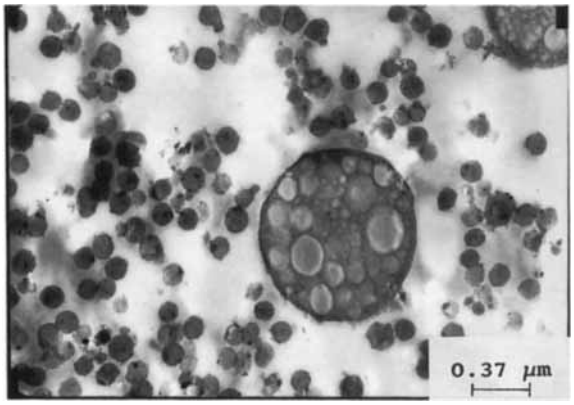

(b)

Figure 1 Injection series materials' microstructures from transmission electron microscopy. (a) ABS 240, (b) ABS 440, (c) ABS 640, and (d) ABS 740.

load-displacement curve by the approximate equation proposed by Rice,[14]

$$J = \frac{2U}{B(W - a)}$$

where the fracture energy, U, is the area under the load deflection curve, and B, W, and a are thickness, width, and initial notch length, respectively.

The amount of crack extension, Δa, for stable crack propagation was postmortem determined from the fracture surface. Δa was evidenced by painting with an alcoholic iodine solution before unloading.

J–R curves were fitted to a simple power law given by

$$J = C_1 \Delta a^{C_2}.$$

The crack initiation values J_{IC} under static conditions were estimated at J at a total crack propagation of 0.2 mm, as recommended by the European Group on Fracture Task of Polymers, to make initiation values independent of yield strength. The initiation values reported for SAN matrixes were calculated from K_{IC} using $J_{IC} = K_{IC}^2/[E(1 - \nu^2)]$ because their fracture was totally elastic and hence, linear elastic fracture mechanics was suitable.

The material resistance to crack propagation, after J_{IC} was exceeded, was characterized by the slope of the J–R curve (dJ/da) and the tearing modulus[15]:

$$T_M = \frac{E}{\sigma^2}\frac{dJ}{da}.$$

As tearing modulus is a material property only close to the onset of stable crack propagation, and aiming to have a single value of dJ/da, T_M was de-

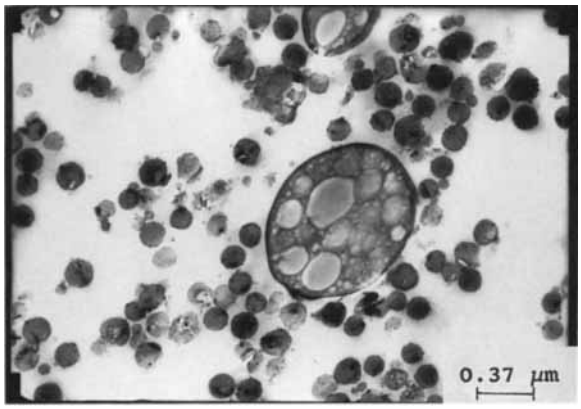

(c)

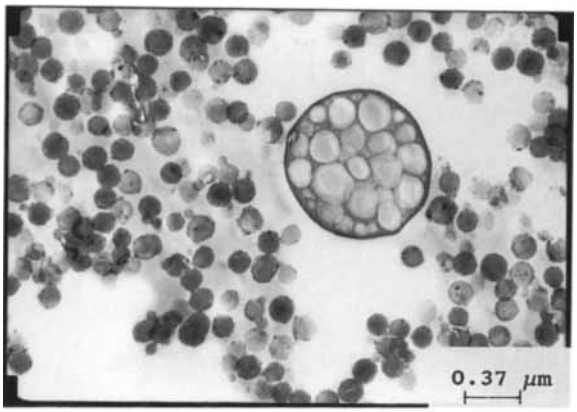

(d)

Figure 1 (*Continued*)

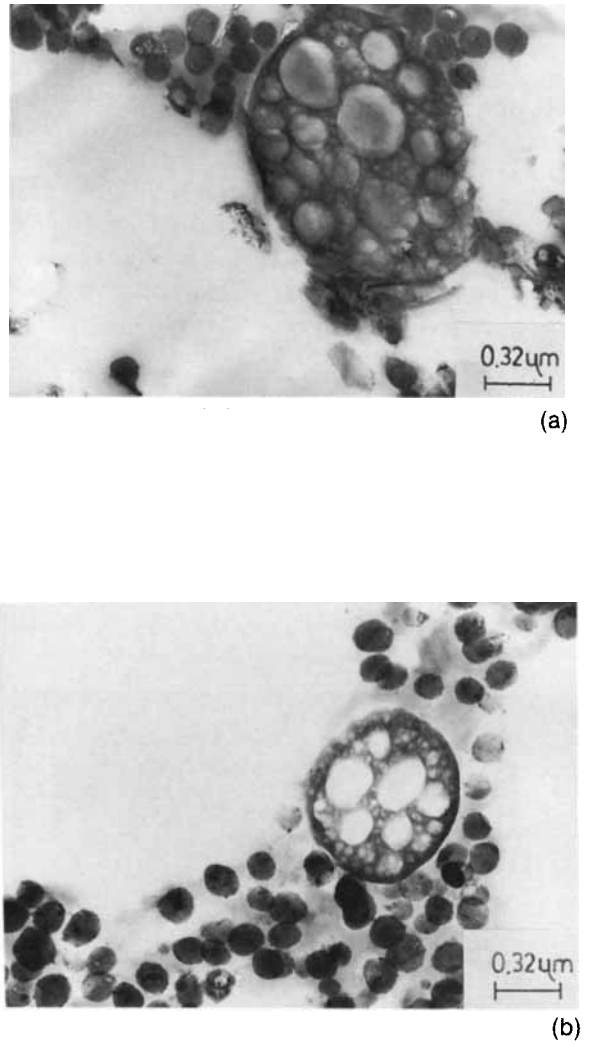

Figure 2 Extrusion series materials' microstructures from transmission electron microscopy. (a) ABS 252 and (b) ABS 452.

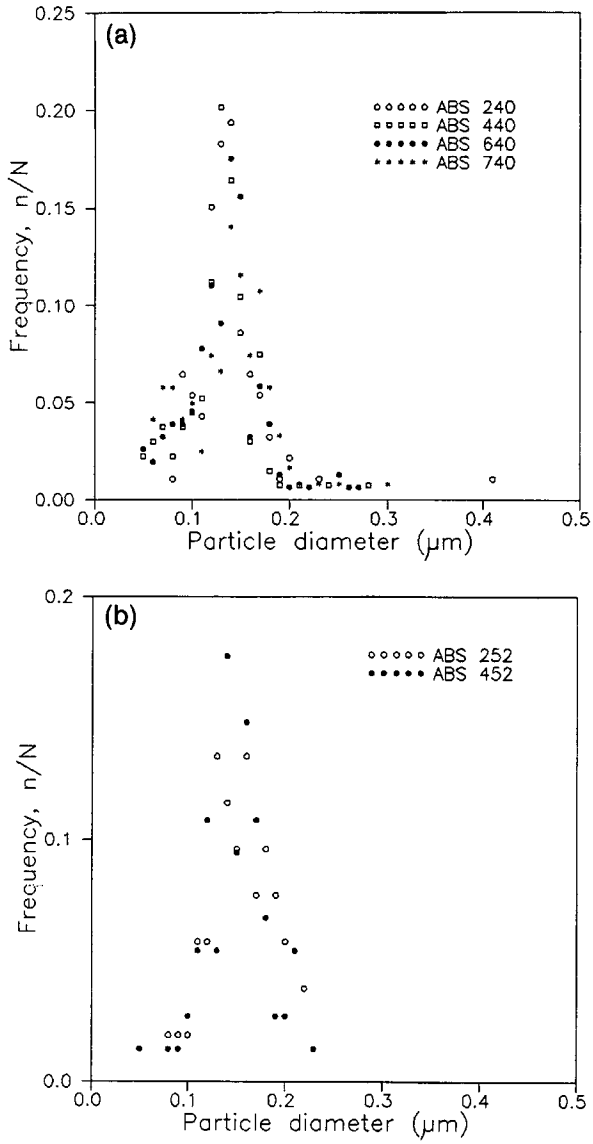

Figure 3 Numerical fraction of particles vs. particle diameter. (a) Injection series and (b) extrusion series.

termined from the linear fitting of the experimental stable crack growth data as proposed by the Metals Standard ASTM E813-81.

The critical initiation parameter under dynamic conditions J_{Cdyn} was determined following the method of analysis proposed by Plati and Williams[16] as the double of the slope of the plot of the energy absorbed in the fracture, U vs. the cross-sectional area of the ligament behind the notch, $B(W - a)$:

$$J_C = \frac{2U}{B(W - a)}.$$

The energy values reported here were corrected by kinetics effects.[17]

RESULTS AND DISCUSSION

Morphology

A qualitative and quantitative examination of TEM photomicrographs of sections of different ABS samples (Figs. 1, 2) showed that in all the materials the dispersed phase consists mainly of small solid particles (emulsion polymerization) with only a few large particles showing glassy polymer subinclusions (mass polymerization).[18–20] These materials displaying both kinds of particles are known as hybrid ABS. The volume fraction of the dispersed phase is the relevant variable in these materials. The average size remains practically constant with the increase in the rubber content and matrix molecular weight

Table II Mechanical Properties vs. Rubber Content for Two ABS Series

Material	Rubber Content (%)	Flexural Modulus (MPa)	Tensile Yield Strength (MPa)	Compressive Yield Strength (MPa)	Charpy Strength (kJ/m^2)
CN 87	0	3095	—	—	2
ABS 240	10.6	2677	48	92	5
ABS 440	15.5	2400	37	74	17
ABS 640	18.0	2149	—	—	26
ABS 740	23.1	1787	32	52	21
CN 88	0	3133	—	—	2
ABS 252	10.6	2751	38	79	9
ABS 452	15.6	2389	34	63	10

[Table I, Fig. 3(a), (b)]. Dillon and Bevis[21] and Braglia and Casiraghi[22] found comparable morphology parameters in other ABS polymers.

Rubber particles appear to be agglomerated with large areas of the matrix devoid of particles. This effect has been explained in the literature[9] in terms of the differences in the acrylonitrile content of the graft SAN and the matrix copolymer that influences their miscibility and consequently the dispersion of the rubbery phase. Moreover, this effect seems to be still more pronounced in the ABS extrusion series that displayed a higher matrix molecular weight. The differences in rubber particle dispersion between these two series could also be due to a lower degree of latex blending induced by higher matrix molecular weight. Overall AN content is practically the same for all the ABS type resins investigated here (Table I).

Deformation and Yield Behavior

Mechanical properties are summarized in Table II.

The small strain behavior, as represented by flexural modulus, is shown in Figure 4(a) and (b) as a function of the initial rubber volume fraction calculated from the added rubber content. Results were practically independent of matrix molecular weight and as expected, a markedly decreasing trend, as rubber content increases, was found. E data points fall between Paul[23] and Ishai-Cohen limits.[24]

In tensile and compressive tests, all samples displayed ductile behavior, exhibiting yield and associated stress whitening. For tensile experiments the load-displacement traces displayed a distinct yield point without further increase in the applied load after yielding. Independent of the matrix molecular weight, a general decreasing trend between yield stress and rubber content was found.

All samples exhibited yield stress values in compression much higher than the ones displayed in tension, in contradiction to previously reported

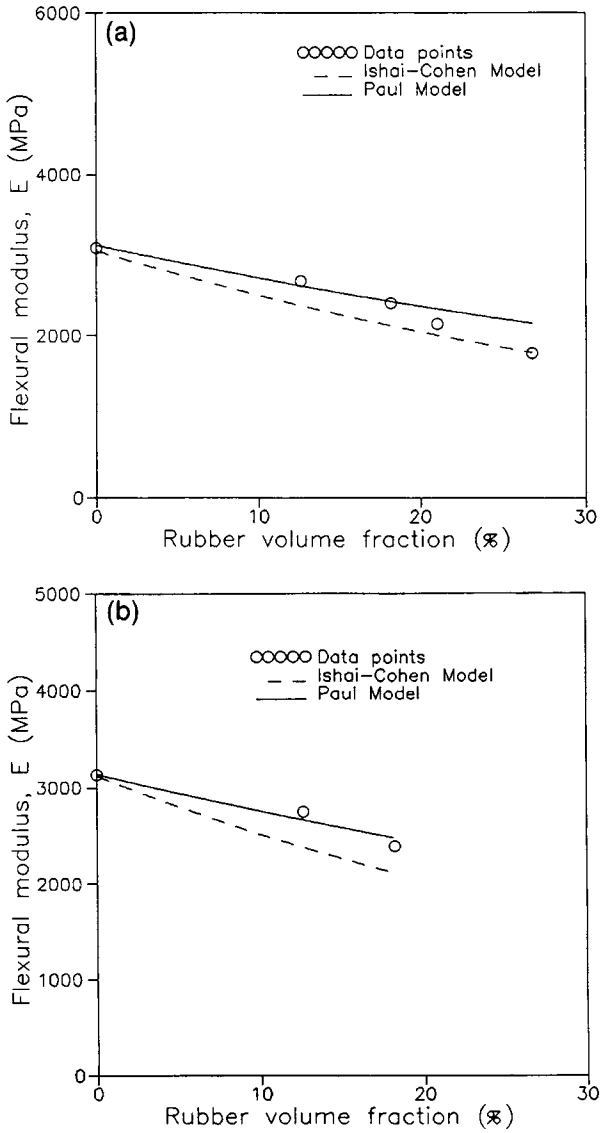

Figure 4 Flexural modulus vs. rubber volume fraction. (a) Injection series and (b) extrusion series.

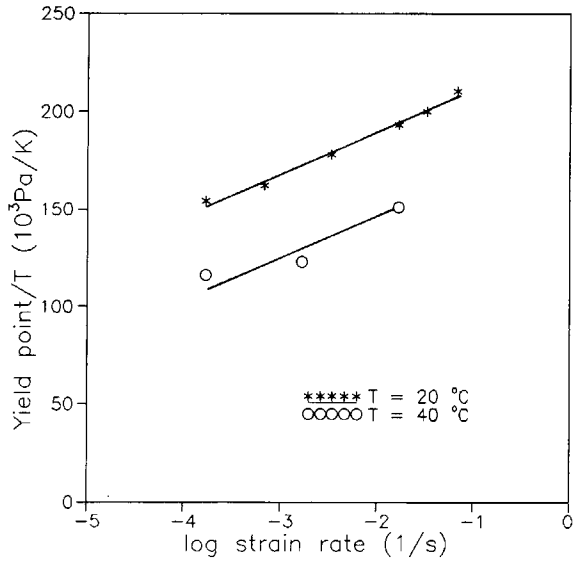

Figure 5 σ_{yt}/T vs. strain rate for Lustran ABS 240. (The Eyring activation energy and volume result 1668.3 A^3 and 45.7 kcal/mol, respectively).

research that showed tensile to compressive yield strength ratio of about 0.75 for many polymers, both thermoplastics and thermosets.[25,26]

Bucknall[27] found a similar result in high-impact polystyrene and he explained the lower σ_{yt}/σ_{yc} value not only in terms of the influence of hydrostatic component upon yield stress in polymers, but also by the fact that crazing is suppressed in compression. Recently Kim et al.,[28] based on dilatometric studies, confirmed that deformation processes in ABS during tensile testing are caused by crazing with possibly some hole formation within the rubber particles, but with little shear yielding.

Contrary to expectations the extrusion series, despite having the highest molecular weight, displayed lower values of σ_y than the ones displayed by the injection series with the same rubber content. This apparently anomalous result may be explained in terms of rubber particle agglomeration. A reduction in yield strength induced by nonuniform dispersions, due to interaction of stress fields between rubber particles at localized regions of high rubber concentrations, was reported in the literature.[28]

ABS 240 tensile strength was also determined for different temperatures and crosshead speeds (Fig. 5). Consistent with previously reported experiments,[29] the experimental data obtained fit the Eyring viscosity equation for a single deformation process in the ranges of temperature and strain rate used. As reported previously,[30,31] the activation energy measured here also lies in the activation energy range reported for crazing or craze yielding. For this reason it is not possible to identify, simply by measuring activation energies, which mechanism of energy absorption (crazing or shear yielding of the matrix) is dominant.

Fracture Evaluation

Fracture characterization results are summarized in Table III. Figure 6(a) and (b) shows J-R stable crack growth curves obtained under static conditions for the two ABS materials series, respectively. Figure 7(a) and (b) shows energy vs. ligament area plots for dynamic experiments.

As expected, the highest matrix toughness was displayed by CN88 which has the highest molecular weight.

The extrusion series exhibited J_C values, under both loading conditions, practically independent of rubber content over 10%. The injection series displayed an analogous result under dynamic conditions above 18% and a weak maximum at about 15% under static conditions. Similar trends were obtained from Charpy impact tests for the same materials as can be observed in Table II. This shows that above certain limits in volume fraction, further incorporation of rubber lowers the modulus of the composite and does not increase the fracture resistance. This inability of the rubber in promoting the toughening mechanism in the matrix is more dramatic in high molecular matrix materials (extrusion series). Similar results were previously found by Dillon and Bevis[32] for ABS having SAN matrices of high molecular weight, and by Bucknall and Faitrouni[33] in fatigue crack growth experiments.

The improvement in toughness with the increase in rubber volume content has been mainly attributed to the increase in number of craze initiation sites and also to differences in matrix/particle adhesion. Recent lap shear measurements indicate that adequate adhesion is obtained over the range of AN contents of the materials tested here,[9] so that this

Table III Fracture Mechanics Parameters

Material	J_{IC} (N/mm)	dJ/da (N/mm^2)	T_M	J_{Cdyn} (N/mm)
CN 87	0.23	—	—	—
ABs 240	4.5	5.2	6.1	18.1
ABS 440	5.9	8.7	14.8	34.0
ABs 640	5.6	6.3	7.2	—
ABS 740	5.0	9.4	16.2	33.4
CN 88	0.43	—	—	—
ABS 252	4.7	6.3	11.8	10.1
ABS 452	5.0	7.4	14.9	10.1

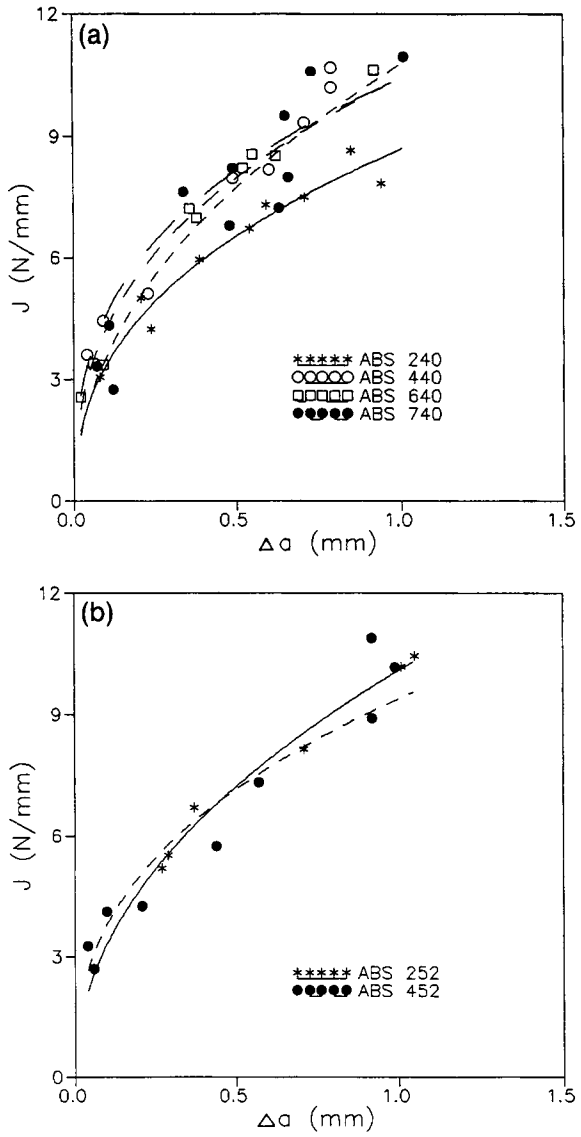

Figure 6 *J–R* curves for ABS polymers. (a) Injection series and (b) extrusion series.

latter effect has not been taken into account in this article.

The capability of the matrix to be toughened appears to be related to matrix molecular weight, because the effectiveness in toughening of crazes is highly related to matrix molecular weight. Chain slip is important in low molecular weight SAN matrixes, but in the higher MWt SAN this mechanism is probably too slow to produce a major contribution, so that fibril failure occurs by chain scission.[32,33]

The weak maximum in toughness displayed by the injection series seems to be principally a consequence of the lower values displayed by the flexural modulus at those rubber contents as reported previously.[7]

The analysis of dJ/da and T_M values (Table III) showed no important differences in materials' resistance to crack propagation after crack initiation for ABS at different rubber contents within each material series. Only ABS 240 displayed a well-defined lower resistance to crack propagation as can be demonstrated from both T_M values and the comparison of J–R curves [Fig. 6(a), (b)].

Variations of Fracture Behavior with Temperature

Fracture behavior for different temperatures was determined on two materials, ABS 740 and ABS 252, under static conditions. Results are shown in Figure 8(a) and (b) and Table IV.

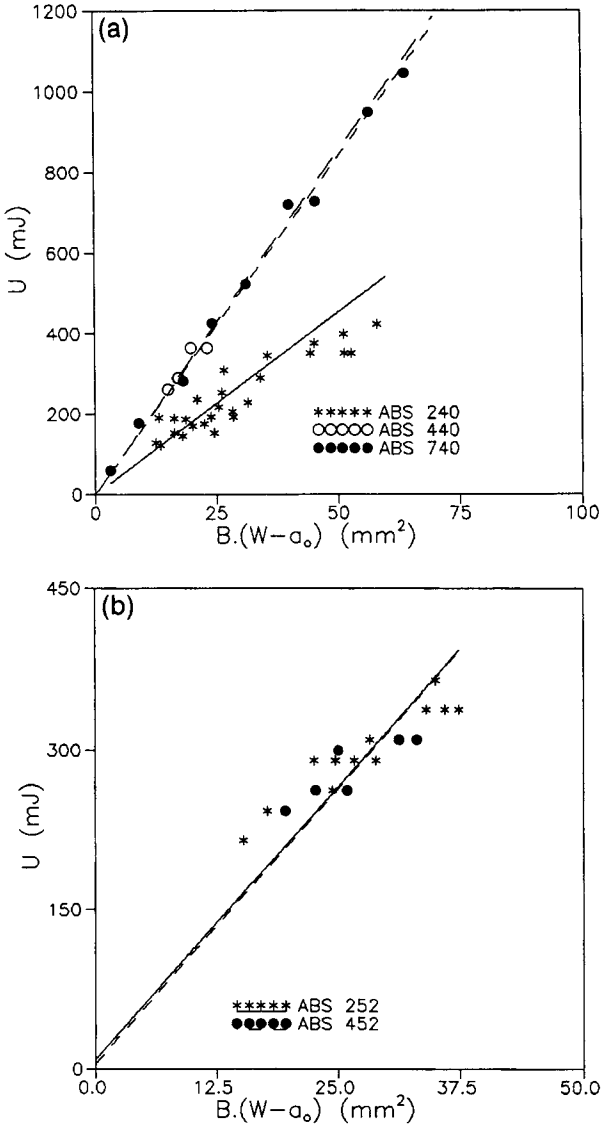

Figure 7 Energy vs. ligament area plots for dynamic experiments. (a) Injection series and (b) extrusion series.

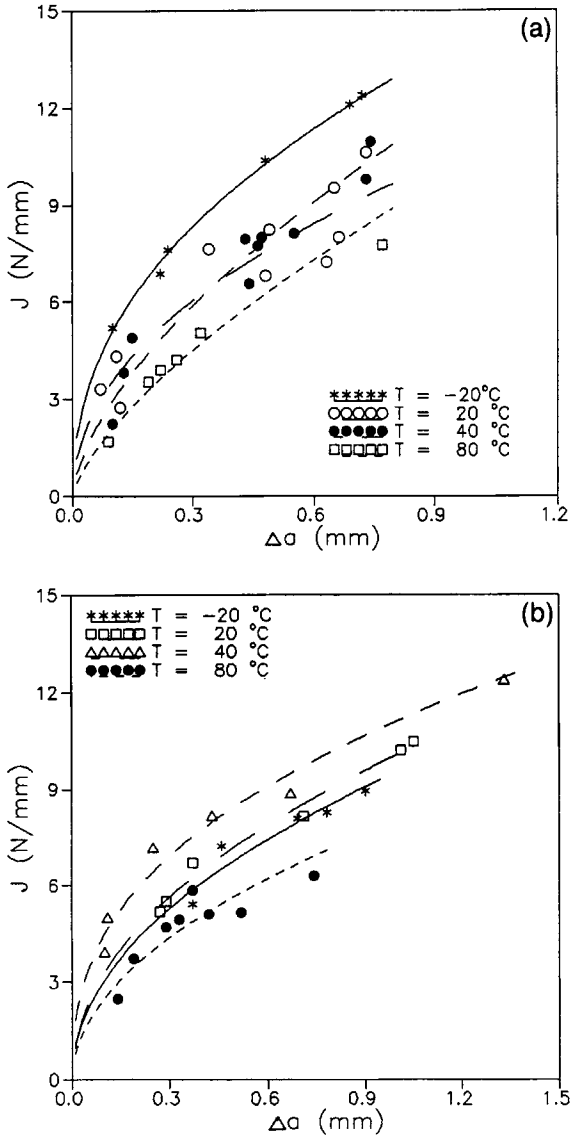

Figure 8 *J-R* curves vs. temperature. (a) ABS 740 and (b) ABS 252.

At every temperature tested, fracture surfaces displayed complete stress whitening and ductile behavior.

ABS 252 displayed a peak fracture toughness at about 40°C, but for both lower and higher temperature, the toughness decreases. ABS 740 displayed a practically continuous decreasing trend with temperature. As Wu et al. suggested,[34] the decrease in toughness with temperature may be explained in terms of competition between the critical crack opening displacement (COD), Δa, and the yield stress, σ_y. If the decrease in yield stress outweighs the increase in COD, the fracture toughness is reduced as temperature is increased. In light of these statements, the monotonic reduction in σ_y with increasing temperature satisfactorily explains the decreasing fracture toughness found with temperature.

Table IV Static Fracture Mechanics Parameters vs. Temperature

Material	Temp. (°C)	J_{IC} (N/mm)	dJ/da (N/mm^2)	T_M
ABS 740	−20	6.9	11.2	11.0
	20	5.0	9.4	16.2
	40	4.6	10.2	21.1
	80	3.4	8.1	34.9
ABS 252	−20	4.3	5.8	4.9
	20	4.7	6.3	11.8
	40	5.9	5.5	15.6
	80	3.6	5.3	26.4

The increase in fracture toughness with temperature displayed by ABS 252 under 40°C may not be attributed to the relaxation process of the rubbery particles in this case. As we worked well above the relaxation temperature of the rubbery phase, it was always active and absorbed considerable energy. Similar behavior was reported by Sridharan and Broutman[5] and was attributed to possible matrix or rubber phases secondary relaxations. Figure 9 shows dynamic mechanical analyses of ABS 252 and ABS 740. In fact ABS 252 displayed a viscoelastic relaxation at about 30°C. The maximum in toughness with temperature seems to also be consistent with the activated nature of crazing that is both time and temperature dependent; as shown previously, the propensity of matrixes with high molecular weights to be toughened seems to be less and so this peak

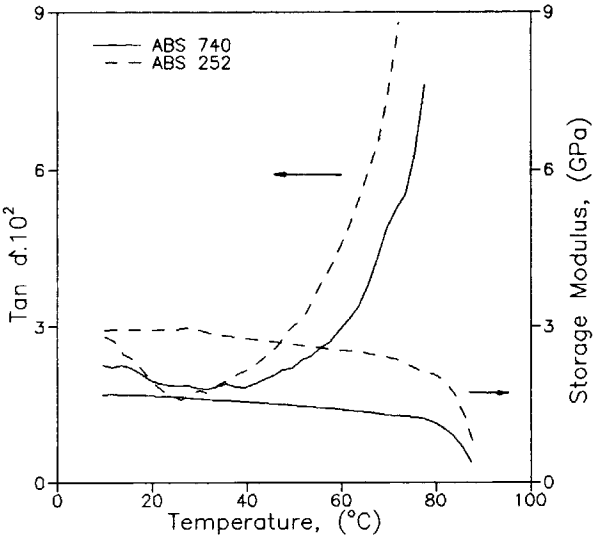

Figure 9 Dynamic mechanical analysis of ABS 252 and ABS 740.

may be related to the fact that crazes in these materials are actually active at higher temperature.

Despite that dJ/da appears to be practically independent of temperature, the tearing modulus shows a well-defined increasing trend with temperature due to the monotonic decreasing trend with temperature displayed by σ_y.

Fractography

Figure 10(a) and (b) shows micrographs of surface fracture of ABS samples fractured under static and dynamic conditions, respectively. The information derived from both pictures suggests that massive cavitation happened inside the rubbery particles as well as in the boundary between the matrix and inclusions. Most of the voids and cavities in this area are several times larger than the original rubbery particles; therefore, it is a reasonable assumption that the coalescence of neighboring voids initiated by individual particles must have occurred.

Besides the cavities formed during void coalescence, Figure 10(a) reveals a more stress whitened and more fibrillated structure that appears to originate from the ductile tearing of the ligament between voids during stable propagation. This indicates that the main deformation events during stable crack propagation seem to be cavitation, void coalescence, and subsequent ductile tearing of the ligaments between voids.

Under impact conditions, however, chain scission is likely to become important. In this case one can speculate that crazing will be favored and voiding and fibrillation will be aided by the scission processes rather than by viscous disentanglement via reptation as occurred in slow strain-rate tests. These observations are consistent with previous investigations.[35] Birkinshaw et al.[36] suggested that the two toughening mechanisms in ABS have different rates of response: ABS tends to deform by shear yielding at low deformation rates and at higher deformation rates crazes and crack fibrillation are more important.

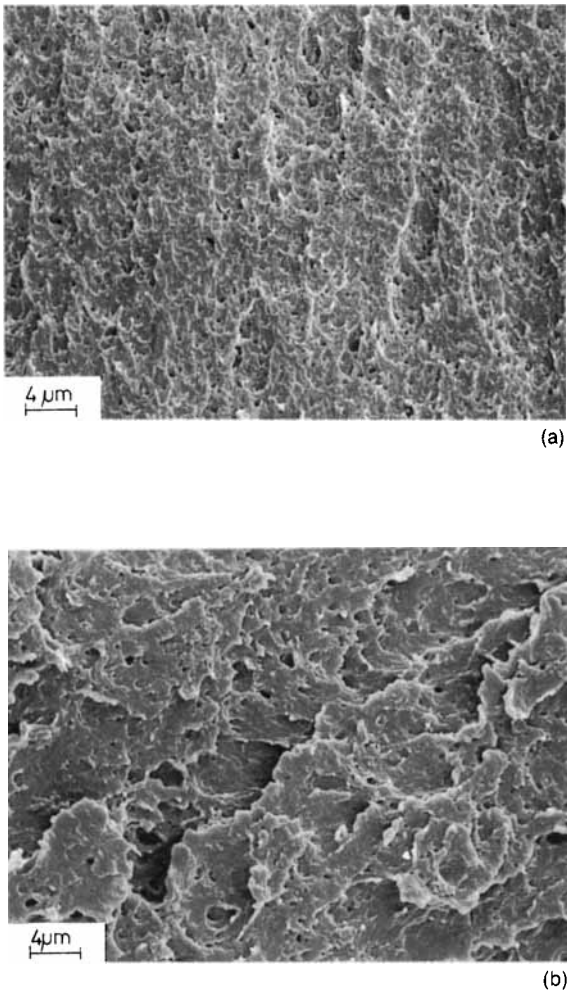

Figure 10 Fracture surface micrographs of ABS samples. (a) Fractured under static conditions and (b) fractured under dynamic conditions.

SUMMARY AND CONCLUSIONS

1. Through the combination of deformation and fracture mechanical investigations, with electron microscopical analysis of morphology and fracture surface structures, a deeper insight into commercial ABS resins behavior was gained.
2. TEM analysis revealed that rubber particles appear to be agglomerated with large areas of the matrix free of particles, especially in samples having large matrix molecular weight, with the dispersed phase consisting mainly of small solid particles with only large particles showing glassy polymers subinclusions.
3. The flexural modulus data points fall between Paul[23] and Ishai–Cohen[24] limits when they are plotted against rubber content.
4. All samples exhibited yield stress values in compression higher than the ones displayed in tension because of the suppression of crazing in compression.
5. The extrusion series displayed lower values of yield strength due to rubber particle agglomeration that induced premature yielding.
6. The Eyring activation energy for Lustran

ABS 240 lies in the activation energy range reported for crazing or craze yielding.

7. The extrusion series exhibits a maximum in J_C at a rubber content of 10% and the injection series at 18 or 15%, depending on the strain rate. The propensity of the matrix to be toughened appears to be related to matrix molecular weight, because the effectiveness in toughening of crazes decreases with the increase in matrix molecular weight.
8. No definite trend between tearing modulus (T_M) and rubber contents was found.
9. ABSs displayed complete stress whitening and ductile behavior over the temperature range tested here (−35–200°C).
10. ABS 252 displayed a peak in toughness with temperature, probably due to the presence of a secondary viscoelastic relaxation or to a lag in crazing activation in high molecular weight matrixes.
11. Our results are consistent with the suggestions of Birkinshaw et al.[36] and Bucknall and coworkers[33] who proposed that the two toughening mechanisms in ABS have different rates of response. At higher rates of strain and at relatively high stresses, crazing and crack fibrillation are more important; and at the lower strain rates encountered in the tensile tests, shear yielding can also play an effective toughening role.

REFERENCES

1. M. Parvin and J. G. Williams, *J. Mater. Sci.*, **11,** 2045 (1976).
2. L. V. Newmann and J. G. Williams, *Polym. Eng. Sci.*, **18,** 893 (1978).
3. H. J. Nusbaum, *J. Mater. Sci. (Lett.)*, **14,** 2755 (1979).
4. L. V. Newmann and J. G. Williams, *J. Mater. Sci.*, **15,** 773 (1980).
5. N. S. Sridharan and L. J. Broutman, *Proc. Int. Conf. Toughening of Plastics I,* London, 1978.
6. R. J. Ferguson, G. P. Marshall, and J. G. Williams, *Polymer,* **14,** 451 (1973).
7. T. Riccó, M. Rink, S. Caporusso, and A. Pavan, *Proc. Int. Conf. Toughening of Plastics II,* London, 1985.
8. H. Keskkula, H. Kim, and D. R. Paul, *Polym. Eng. Sci.*, **30,** 1373 (1990).
9. H. Kim, H. Keskkula, and D. R. Paul, *Polymer,* **31,** 869 (1990).
10. S. Hashemi and J. G. Williams, *Polym. Eng. Sci.*, **26,** 760 (1986).
11. C. R. Bernal, P. M. Frontini, and R. Herrera, *Polym. Testing,* **11,** 271 (1992).
12. S. Hashemi and J. G. Williams, *J. Mater. Sci.*, **26,** 621 (1991).
13. M. J. Zhang, F. X. Zhi, and X. R. Su, *Polym. Eng. Sci.*, **29,** 1142 (1989).
14. J. R. Rice, *J. Appl. Mech.*, **35,** 379 (1968).
15. P. C. Paris, H. Tada, A. Zahoor, and H. Ernst, *Elastic Plast. Fracture, ASTM STP 668,* ASTM, Philadelphia, 1979, p. 5.
16. E. Plati and J. G. Williams, *Polym. Eng. Sci.*, **15,** 470 (1975).
17. D. R. Ireland, *Instrumented Impact Testing, ASTM STP 563,* ASTM, Philadelphia, 1973, p. 7.
18. L. Castellani, R. Frassine, A. Pavan, and M. Rink, *Proc. Int. Conf. Toughening of Plastics III,* London, 1994.
19. A. Echte, in *Rubber Toughened Plastics,* C. K. Riew, Ed., American Chemical Society, Washington, DC, 1982, p. 15.
20. B. S. Lombardo, H. Keskkula, and D. R. Paul, *J. App. Polym. Sci.*, **54,** 1697 (1994).
21. M. Dillon and M. Bevis, *J. Mater. Sci.*, **17,** 1903 (1982).
22. R. Braglia and T. Casiraghi, *J. Mater. Sci.*, **19,** 2643 (1984).
23. B. Paul, *Trans. Am. Inst. Mech. Eng.*, **36,** 218 (1960).
24. O. Ishai and L. J. Cohen, *Int. J. Mech. Sci.*, **9,** 539 (1967).
25. A. S. Wronski and M. Pick, *J. Mater. Sci.*, **12,** 28 (1977).
26. R. H. Sigley, A. S. Wronski, and T. V. Parry, *J. Mater. Sci.*, **26,** 385 (1991).
27. C. B. Bucknall, *Toughened Plastics,* Applied Science Publ., London, 1977, p. 232.
28. H. Kim, H. Keskula, and D. R. Paul, *Polymer,* **32,** 1447 (1991).
29. R. S. Moore and C. Gieniewski, *Polym. Eng. Sci.*, **9,** 190 (1969).
30. R. W. Truss and G. A. Chadwick, *J. Mater. Sci.*, **11,** 111 (1976).
31. R. N. Haward, B. M. Murphy, and E. F. T. White, *Fracture,* Chapman & Hall, London, 1961, p. 519.
32. M. Dillon and M. Bevis, *J. Mater. Sci.*, **17,** 1895 (1982).
33. C. B. Bucknall and T. Faitrouni, 8th Int. Conf. Deformation and Fracture of Polymers, Cambridge, UK, 1991.
34. J. Wu, Y.-W. Mai, and B. Cotterel, *J. Mater. Sci.*, **28,** 3373 (1993).
35. C. Maestrini, L. Castellani, M. Merlotti, and M. Vighi, *Polymer,* **33,** 1556 (1992).
36. C. Birkinshaw, M. Buggy, and F. Quigley, *J. Appl. Polym. Sci.*, **48,** 181 (1993).

Received August 5, 1994
Accepted September 20, 1994